

Supporting Information

Zeolitic Imidazolate Framework-67 Derived CoP/Co@N, P-Doped Carbon
Nanoparticle Composites with Graphitic Carbon Nitride for Enhanced Photocatalytic
Production of H₂ and H₂O₂

*Qingjie Ji^a, Longhai Pan^a, Jixiang Xu^{*a}, Chao Wang^a, Lei Wang^{*a}*

^aKey Laboratory of Eco-Chemical Engineering, Taishan Scholar Advantage and Characteristic Discipline, Team of Eco Chemical Process and Technology, College of Chemistry and Molecular Engineering, Qingdao University of Science and Technology, Qingdao 266042, China

Corresponding authors

E-mail: xujix47@163.com (J.-x. X.)

E-mail: inorchemwl@126.com (L. W.)

Characterization. Powder X-ray diffraction (XRD) data were gathered on a Rigaku D-MAX 2500/PC diffractometer. X-ray photoelectron spectra (XPS) were collected on a X-ray photoelectron spectrometer (Thermo Scientific, K α) equipped with a monochromatic Al K α X-ray source ($h\nu = 1486.6$ eV). UV-vis diffuse reflectance spectra were collected on a Lambda 750 UV/VIS/NIR spectrometer. The morphology of the samples was observed by scanning electron microscopy (SEM) on a TESCAN-VEGA3 instrument. High-resolution transmission electron microscopy (HR-TEM) images were acquired on a Tecnai-G²-F30 high-resolution transmission electron microscope (FEI Company, USA). The photoluminescence (PL) spectra were obtained by a fluorescence-spectrophotometer (F-4500 FL). Ultraviolet photoelectron spectroscopy (UPS) were investigated by a VG Scienta R4000 analyzer having a monochromatic He I light source (21.2 eV). A sample bias of -5 V was applied to obtain the secondary electron cutoff (SEC). The electron spin response (ESR) signal of $\cdot\text{O}_2^-$ was observed by a JEOL JES-FA200 spectrometer, and 5,5-dimethyl-1-pyrroline N-oxide (DMPO) was used as spin-trapped reagent. The time-resolved photoluminescence (TRPL) spectra were collected by an Edinburgh FLS920 fluorescence spectrofluorometer.

Photocatalytic activity for H₂ and H₂O₂ production. The H₂ evolution was performed in a quartz flask equipped with a flat optical entry window. 10 mg of the obtained photocatalysts was added into 100 mL 15% triethanolamine (TEOA) aqueous solution, and the system was deaerated by bubbling N₂ for 30 min before turn on the light. A 300-W Xe lamp with cut-off filter ($\lambda > 420$ nm) was employed as the

visible-light source. The amount of H₂ produced was determined using an online gas chromatography system (GC-7920). The apparent quantum efficiency (AQE) was determined under the same photocatalytic reaction conditions. The reaction mixtures were irradiated for 60 min. AQE can be calculated using the following equation:

$$\text{AQE} = \frac{2 \times \text{the number of evolved hydrogen molecules}}{\text{the number of incident photons}} \times 100\%$$

For photocatalytic H₂O₂ production, 10 mg of the photocatalyst was added into 50 mL 10% isopropanol (IPA) aqueous solution or ultrapure water. Then O₂ was continually bubbled to achieve saturation adsorption before turn on the light. The suspension was illuminated by simulated sunlight (filter: AM1.5). 3 mL of the dispersion was collected at regular time. The produced H₂O₂ concentration was determined by iodometry.¹ The AQE was calculated using the equation:

$$\text{AQE} = \frac{2 \times \text{the number of evolved hydrogen peroxide molecules}}{\text{the number of incident photons}} \times 100\%$$

Photoelectrochemical measurements. The electrochemical impedance spectra (EIS) and photocurrent measurements were collected on a standard three-electrode electrochemical analyzer (PEC2000, Beijing). The FTO electrode coated with samples was acted as the working electrode, an Ag/AgCl (saturated KCl) as the reference electrode, and a Pt foil as the counter electrode. A 300-W Xe arc lamp (PLS-SXE300) was employed as the light source. A 0.5 M Na₂SO₄ solution was employed as the electrolyte. The working electrodes were prepared according to previous work.²

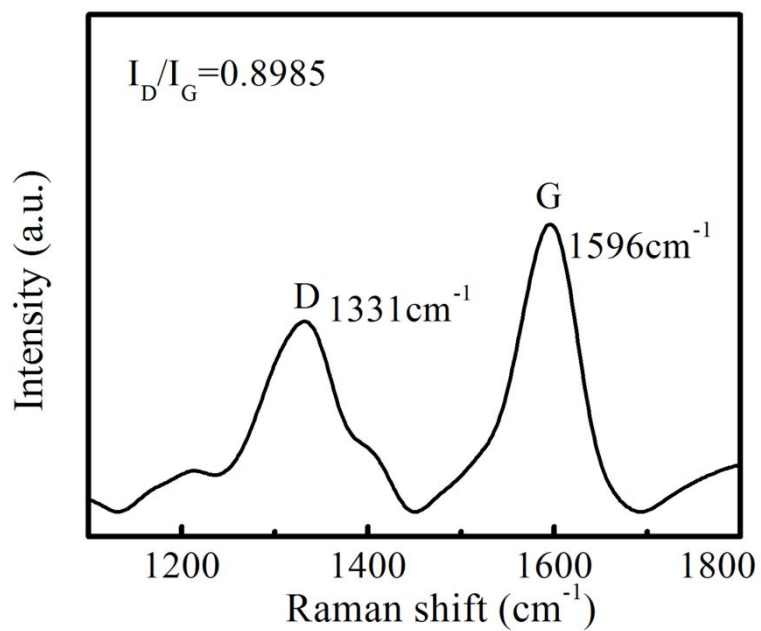


Figure S1. The Raman spectrum of Co@NC composite.

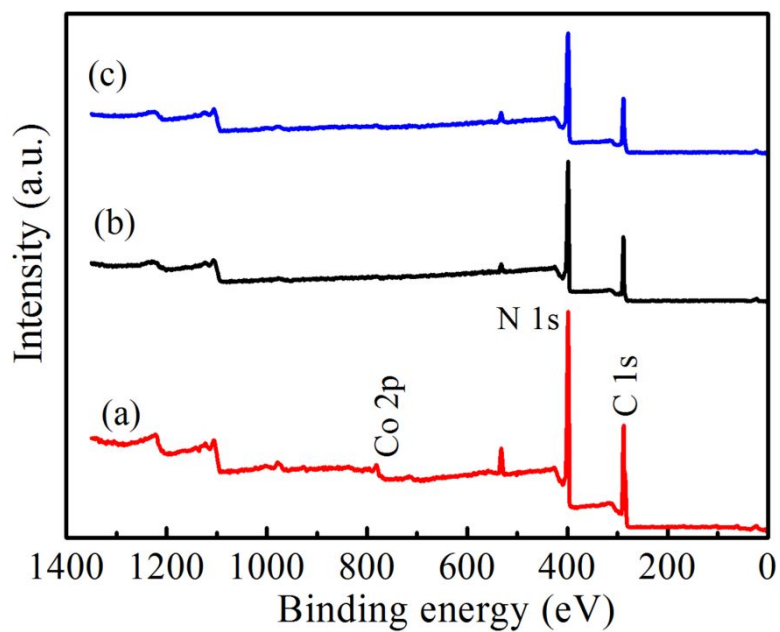


Figure S2. The XPS survey spectra of fresh (a) and used CoP/Co@NPC-15/g-C₃N₄ photocatalyst after H₂O₂ (b) and H₂ (c) production.

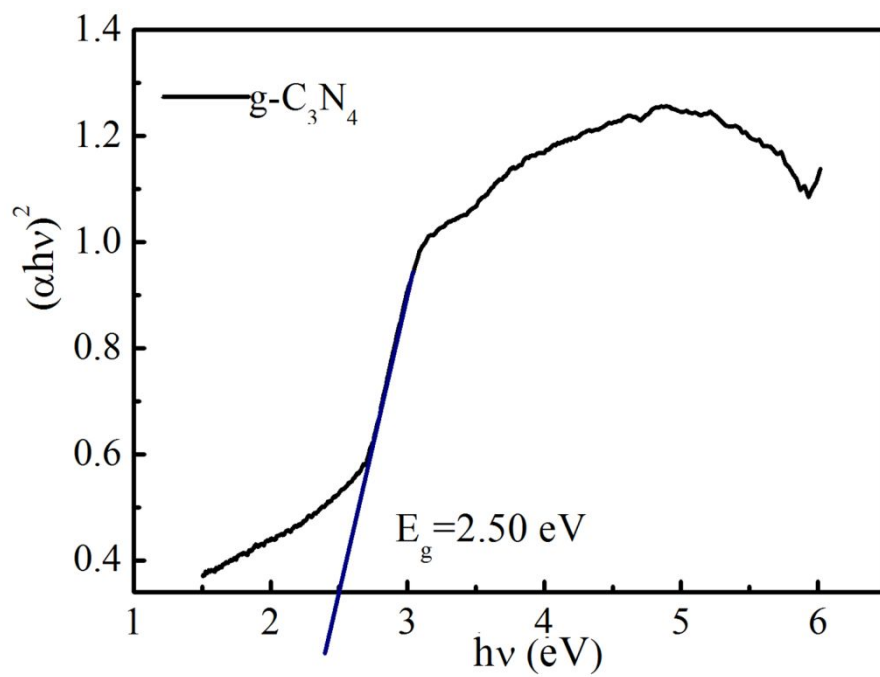


Figure S3. $(\alpha h\nu)^2$ vs radiation energy ($h\nu$) plot for g-C₃N₄.

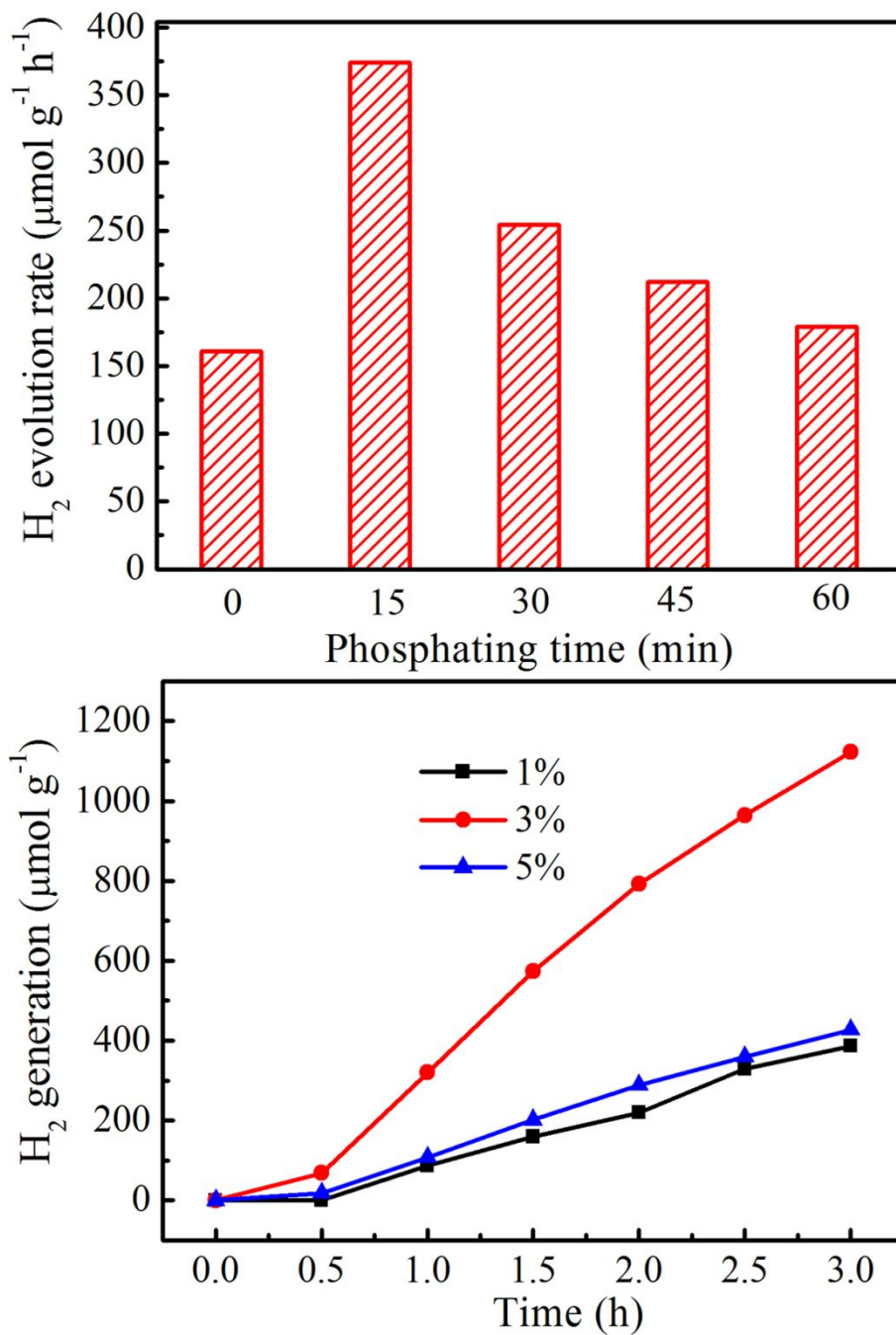


Figure S4. H₂ evolution rate over (a) Co@NC/g-C₃N₄ and CoP/Co@NPC/g-C₃N₄ after phosphidation for 15, 30, 45, and 60 min (upper); Effects of CoP/Co@NPC-15 dosage on photocatalytic H₂ evolution performance of g-C₃N₄ (below).

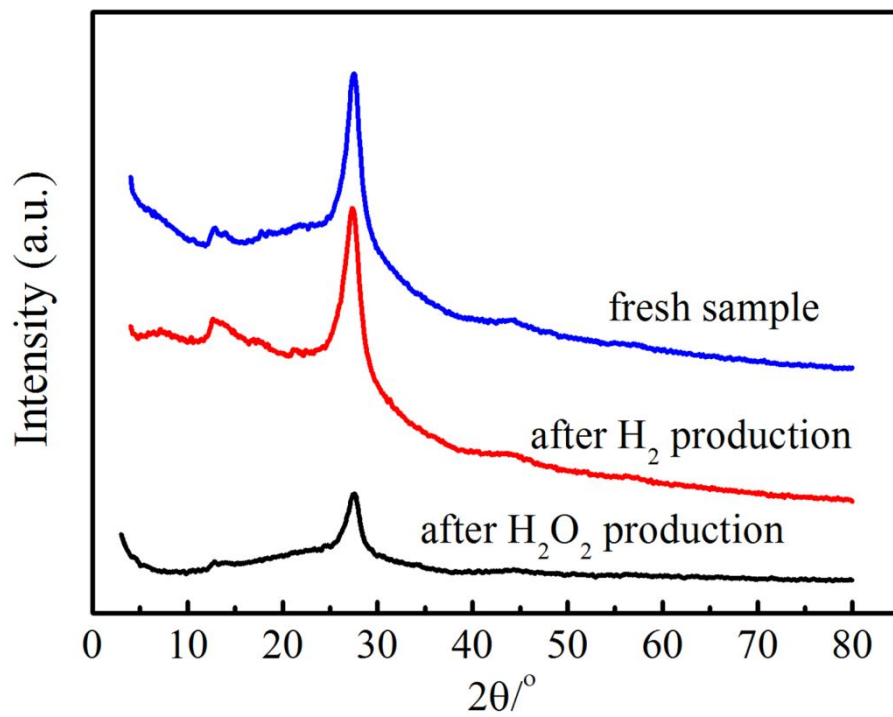


Figure S5. XRD patterns of fresh and used CoP/Co@NPC-15/g-C₃N₄ photocatalyst.

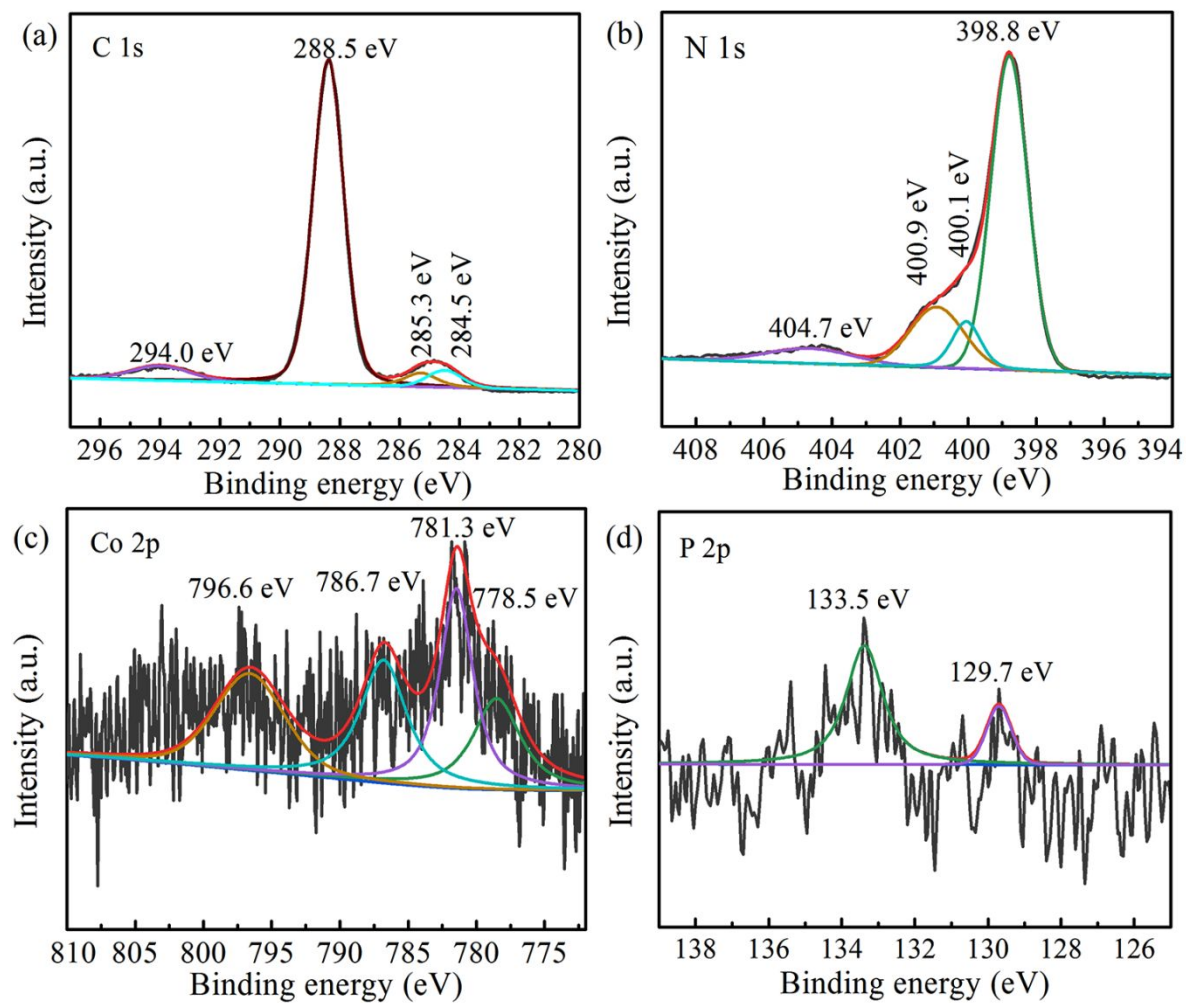


Figure S6. High-resolution XPS spectra of (a) C 1s, (b) N 1s, (c) Co 2p, and (d) P 2p

in CoP/Co@NPC-15/g-C₃N₄ photocatalyst after H₂ production.

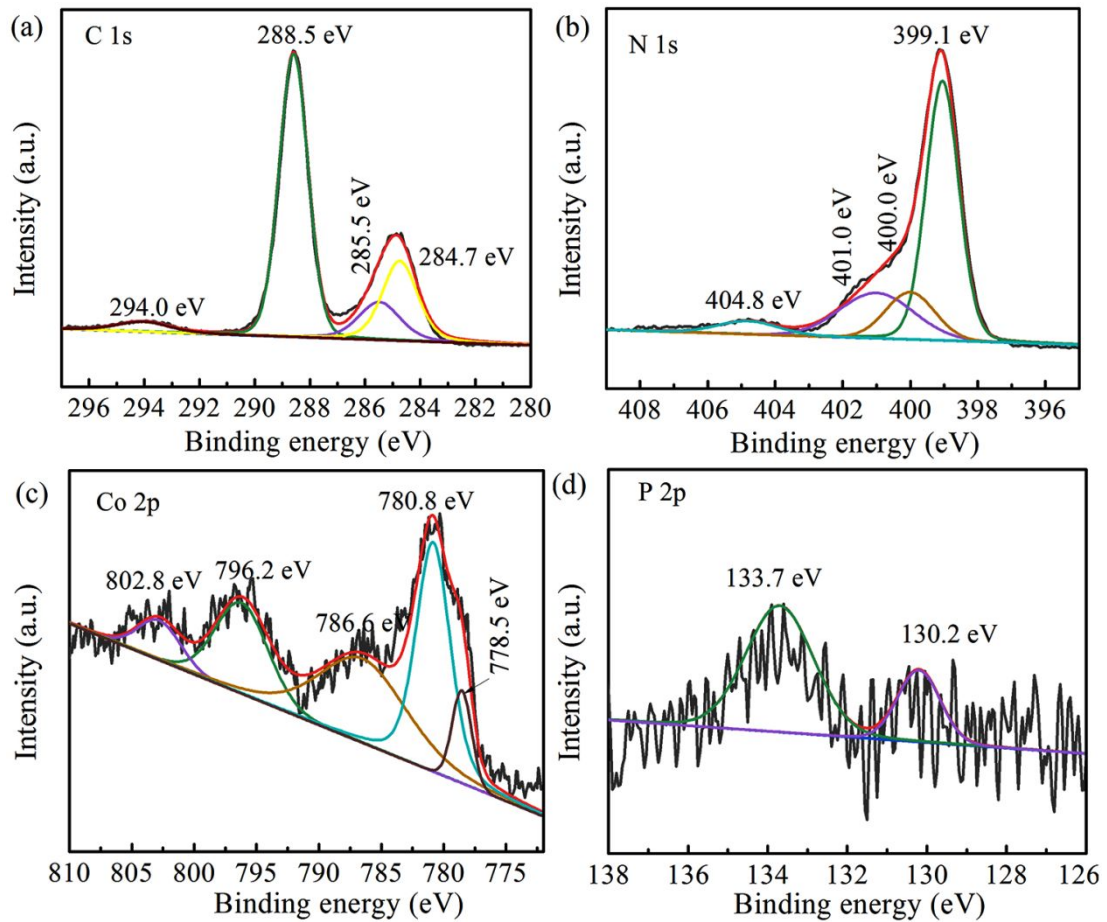


Figure S7. High-resolution XPS spectra of (a) C 1s, (b) N 1s, (c) Co 2p, and (d) P 2p in CoP/Co@NPC-15/g-C₃N₄ photocatalyst after H₂O₂ production.

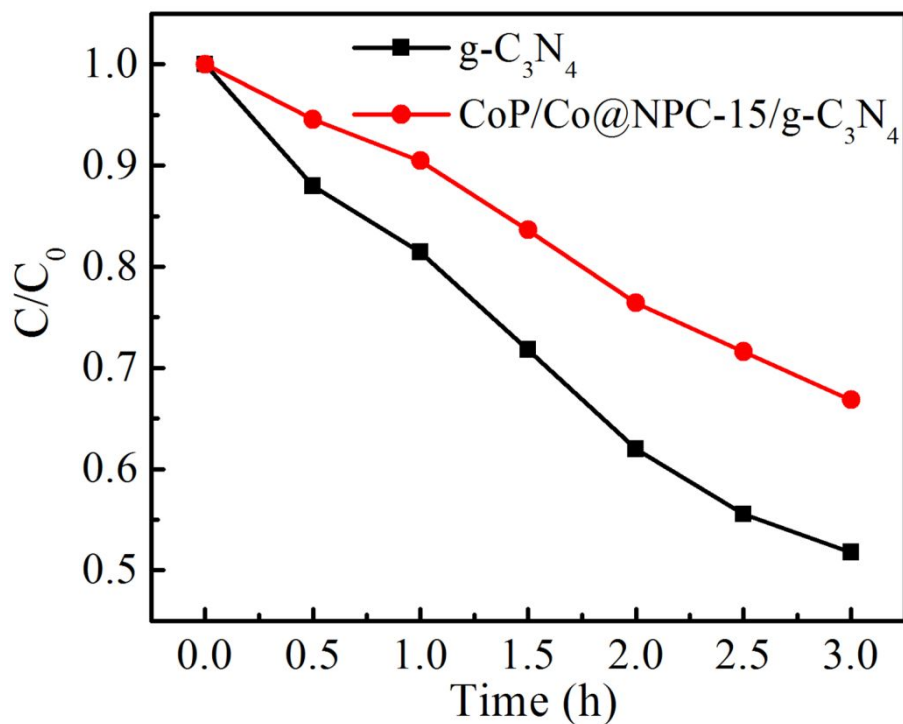


Figure S8. The photocatalytic decomposition of H₂O₂ (1 mmol L⁻¹) under visible light irradiation

Table S1. Comparison of photocatalytic H₂ evolution rates of various cocatalyst modified g-C₃N₄ photocatalysts.

Photocatalysts	Maximum rate ($\mu\text{mol h}^{-1} \text{g}^{-1}$)	photocatalyst dosage/mg	Scavenger	Light source (Xe lamp)	Reference
3%CoP/Co@NPC-15/g-C ₃ N ₄	374.1	10	15% TEOA	$\lambda > 420 \text{ nm}$	This work
g-C ₃ N ₄ -3%Ni ₃ B-2%Ni(OH) ₂	352.43	50	15% TEOA	$\lambda > 420 \text{ nm}$	3
40%Co@CNT/g-C ₃ N ₄	1208	20	20% TEOA	Au Light, $\lambda > 420 \text{ nm}$	4
2.0 wt.% Mo-Mo ₂ C/g-C ₃ N ₄	219.7	5	10% TEOA	$\lambda > 420 \text{ nm}$	5
3%Ag-Cu/g-C ₃ N ₄	246	40	10% TEA	$\lambda > 420 \text{ nm}$	6

15% MoO ₂ -C/g-C ₃ N ₄	1070	10	10% TEOA	$\lambda > 400$ nm	7
g-C ₃ N ₄ /0.5%graphene/1.2% MoS ₂	317	50	0.1 mol L ⁻¹ TEOA	$\lambda > 420$ nm	8
g-C ₃ N ₄ -0.5% carbon black-1.0%NiS	366.4	50	15 % TEOA	$\lambda > 420$ nm	9
g-C ₃ N ₄ -1%Ni ₂ P-1.5%MoS ₂	532.14	25	15 % TEOA	$\lambda > 400$ nm	10
1%NiS/P-S codoped g-C ₃ N ₄	305	100	20% TEOA	$\lambda > 400$ nm	11
g-C ₃ N ₄ -0.5% acetylene black-2%CuS	348	50	10 % TEOA	$\lambda > 420$ nm	12
g-C ₃ N ₄ /0.52%MoS ₂ /3.18% red phosphorus	257.9	10	10 % TEOA	$\lambda > 420$ nm	13
g-C ₃ N ₄ /2%CoMoS ₂ /5%rGO	684	100	20 % TEOA	$\lambda > 400$ nm	14

Table S2. Comparison of photocatalytic H₂O₂ evolution rates of various g-C₃N₄ based photocatalysts.

Photocatalysts	H ₂ O ₂ production activity (μmol h ⁻¹ g ⁻¹)	catalyst dosage/mg	Reaction solution	Light source	Reference
3%CoP/Co@NPC-15/g-C ₃ N ₄	940	10	10% IPA(50mL)	AM 1.5G	This work
1.76 wt%CoP/g-C ₃ N ₄	70	20	10% ethanol(20mL)	λ > 420 nm	15
Co ₃ O ₄ /g-C ₃ N ₄	3780	20	water(20mL)	λ > 420 nm	16
Ag@U-g-C ₃ N ₄ -NS	67.50	100	water(100mL)	λ > 420 nm	17
P-porous g-C ₃ N ₄	1083	50	5% ethanol(50mL)	AM 1.5G	18
Reduced g-C ₃ N ₄	170	100	water(100mL)	λ > 420 nm	19
Ti ₃ C ₂ Mxene/porous g-C ₃ N ₄	131.71	50	10% IPA (50mL)	λ > 420 nm	20
Cu ₂ (OH)PO ₄ /g-C ₃ N ₄	1200	200	water(200mL)	λ > 800 nm	21
SiW ₁₁ /g-C ₃ N ₄	152	100	5% methanol(100mL)	AM 1.5G	22
Au/g-C ₃ N ₄	330	30	5% IPA(30mL)	λ > 420 nm	23
Holey defective g-C ₃ N ₄	96.8	50	20% IPA(60mL)	AM 1.5G	24
K-doped g-C ₃ N ₄	473	100	10% ethanol (100 mL)	λ > 420 nm	25

Reference

- (1) Wei, Z.; Liu, M. L.; Zhang, Z. J.; Yao, W. Q.; Tan, H. W.; Zhu, Y. F. Efficient visible-light-driven selective oxygen reduction to hydrogen peroxide by oxygen-enriched graphitic carbon nitride polymers. *Energy Environ. Sci.* **2018**, *11*, 2581–2589.
- (2) Xu, J. X.; Qi, Y. H.; Wang, L. In situ derived Ni₂P/Ni encapsulated in carbon/g-C₃N₄ hybrids from metal–organic frameworks/g-C₃N₄ for efficient photocatalytic hydrogen evolution. *Appl. Catal. B: Environ.* **2019**, *246*, 72–81.
- (3) Lu, X. Y.; Xie, J.; Liu, S. Y.; Adamski, A.; Chen, X. B.; Li, X. Low-cost Ni₃B/Ni(OH)₂ as an ecofriendly hybrid cocatalyst for remarkably boosting photocatalytic H₂ production over g-C₃N₄ nanosheets. *ACS Sustainable Chem. Eng.* **2018**, *6*, 13140–13150.
- (4) Liu, Q. X.; Zeng, C. M.; Xie, Z. H.; Ai, L. H.; Liu, Y. Y.; Zhou, Q.; Jiang, J.; Sun, H. Q.; Wang, S. B. Cobalt@nitrogen-doped bamboo-structured carbon nanotube to boost photocatalytic hydrogen evolution on carbon nitride. *Appl. Catal. B: Environ.* **2019**, *254*, 443–451.
- (5) Dong, J.; Shi, Y.; Huang, C. P.; Wu, Q.; Zeng, T.; Yao, W. F. A New and stable Mo-Mo₂C modified g-C₃N₄ photocatalyst for efficient visible light photocatalytic H₂ production. *Appl. Catal. B: Environ.* **2019**, *243*, 27–35.
- (6) Zhu, Y. X.; Marianov, A.; Xu, H. M.; Lang, C.; Jiang, Y. J. Bimetallic Ag-Cu supported on graphitic carbon nitride nanotubes for improved visible-light photocatalytic hydrogen production. *ACS Appl. Mater. Interfaces* **2018**, *10*, 9468–9477.

- (7) Chen, Z. G.; Xia, K. X.; She, X. J.; Mo, Z.; Zhao, S. W.; Yi, J. J.; Xu, Y. G.; Chen, H. X.; Xu, H.; Li, H. M. 1D metallic MoO₂-C as co-catalyst on 2D g-C₃N₄ semiconductor to promote photocatalytic hydrogen production. *Appl. Surf. Sci.* **2018**, *447*, 732–739.
- (8) Yuan, Y. J.; Yang, Y.; Li, Z. J.; Chen, D. Q.; Wu, S. T.; Fang, G. L.; Bai, W. F. Promoting charge separation in g-C₃N₄/graphene/MoS₂ photocatalysts by two-dimensional nanojunction for enhanced photocatalytic H₂ production. *ACS Appl. Energy Mater.* **2018**, *1*, 1400–1407.
- (9) Wen, J. Q.; Xie, J.; Yang, Z. H.; Shen, R. C.; Li, H. Y.; Luo, X. Y.; Chen, X. B.; Li, X. Fabricating the robust g-C₃N₄ nanosheets/carbons/NiS multiple heterojunctions for enhanced photocatalytic H₂ generation: an insight into the trifunctional roles of nanocarbons. *ACS Sustainable Chem. Eng.* **2017**, *5*, 2224–2236.
- (10) Lu, X. Y.; Xie, J.; Chen, X. B.; Li, X. Engineering MP_x (M = Fe, Co or Ni) interface electron transfer channels for boosting photocatalytic H₂ evolution over g-C₃N₄/MoS₂ layered heterojunctions. *Appl. Catal. B: Environ.* **2019**, *252*, 250–259.
- (11) Liu, L. P.; Xu, X. J.; Si, Z. C.; Wang, Z. H.; Ran, R.; He, Y. H.; Weng, D. Noble metal-free NiS/P-S codoped g-C₃N₄ photocatalysts with strong visible light absorbance and enhanced H₂ evolution activity. *Catal. Commun.* **2018**, *106*, 55–59.
- (12) Shen, R. C.; Xie, J.; Guo, P. Y.; Chen, L. S.; Chen, X. B.; Li, X. Bridging the

- g-C₃N₄ nanosheets and robust CuS cocatalysts by metallic acetylene black interface mediators for active and durable photocatalytic H₂ production. *ACS Appl. Energy Mater.* **2018**, *1*, 2232–2241.
- (13) Zhao, H.; Sun, S. N.; Wu, Y.; Jiang, P. P.; Dong, Y. M.; Xu, Z. C. Ternary graphitic carbon nitride/red phosphorus/molybdenum disulfide heterostructure: An efficient and low cost photocatalyst for visible-light-driven H₂ evolution from water. *Carbon.* **2017**, *119*, 56–61.
- (14) Xu, X.; Si, Z.; Liu, L.; Wang, Z.; Chen, Z.; Ran, R.; He, Y.; Weng, D. CoMoS₂/rGO/C₃N₄ ternary heterojunctions catalysts with high photocatalytic activity and stability for hydrogen evolution under visible light irradiation. *Appl. Surf. Sci.* **2018**, *435*, 1296–1306.
- (15) Peng, Y. L.; Wang, L. Z.; Liu, Y. D.; Chen, H. J.; Lei, J. Y.; Zhang, J. L. Visible-light-driven photocatalytic H₂O₂ production on g-C₃N₄ loaded with CoP as a noble metal free cocatalyst. *Eur. J. Inorg. Chem.* **2017**, *2017*, 4797–4802.
- (16) Zhu, C.; Zhu, M. M.; Sun, Y.; Zhou, Y. J.; Gao, J.; Huang, H.; Liu, Y.; Kang, Z. H. Carbon supported oxygen vacancy-rich Co₃O₄ for robust photocatalytic H₂O₂ production via coupled water oxidation and oxygen reduction reaction. *ACS Appl. Energy Mater.* **2019**, *2*, 8737–8746.
- (17) Cai, J. S.; Huang, J. Y.; Wang, S. C.; Iocozzia, J.; Sun, Z. T.; Sun, J. Y.; Yang, Y. K.; Lai, Y. K.; Lin, Z. Q. Crafting mussel-inspired metal nanoparticle-decorated ultrathin graphitic carbon nitride for the degradation of chemical pollutants and production of chemical resources. *Adv. Mater.* **2019**, *31*, 1806314–1806324.

- (18) Zhou, L.; Feng, J. R.; Qiu, B. C.; Zhou, Y.; Lei, J. Y.; Xing, M. Y.; Wang, L. Z.; Zhou, Y. B.; Liu, Y. D.; Zhang, J. L. Ultrathin g-C₃N₄ nanosheet with hierarchical pores and desirable energy band for highly efficient H₂O₂ production. *Appl. Catal. B: Environ.* **2020**, *267*, 118396–118426.
- (19) Zhua, Z. D.; Pana, H. H.; Muruganathanb, M.; Gongga, J. Y.; Zhanga, Y. R. Visible light-driven photocatalytically active g-C₃N₄ material for enhanced generation of H₂O₂. *Appl. Catal. B: Environ.* **2018**, *232*, 19–25.
- (20) Yang, Y.; Zeng, Z. T.; Zeng, G. M.; Huang, D. L.; Xiao, R.; Zhang, C.; Zhou, C. Y.; Xiong, W. P.; Wang, W. J.; Cheng, M.; Xue, W. J.; Guo, H.; Tang, X.; He, D. H. Ti₃C₂ Mxene/porous g-C₃N₄ interfacial Schottky junction for boosting spatial charge separation in photocatalytic H₂O₂ production. *Appl. Catal. B: Environ.* **2019**, *258*, 117956–117966.
- (21) Wang, X. W.; Han, Z.; Yu, L. H.; Liu, C. T.; Liu, Y. F.; Wu, G. Synthesis of full-spectrum-response Cu₂(OH)PO₄/g-C₃N₄ photocatalyst with outstanding photocatalytic H₂O₂ production performance via a “two channel route”. *ACS Sustainable Chem. Eng.* **2018**, *6*, 14542–14553.
- (22) Zhao, S.; Zhao, X.; Ouyang, S. X.; Zhu, Y. F. Polyoxometalates covalent combined with graphitic carbon nitride for photocatalytic hydrogen peroxide production. *Catal. Sci. Technol.* **2018**, *8*, 1686–1695.
- (23) Chang, X. Y.; Yang, J. J.; Han, D. D.; Zhang, B.; Xiang, X.; He, J. Enhancing light-driven production of hydrogen peroxide by anchoring Au onto C₃N₄. *Catalysts* **2018**, *8*, 147–159.

- (24) Shi, L.; Yang, L. Q.; Zhou, W.; Liu, Y. Y.; Yin, L. S.; Hai, X.; Song, H.; Ye, J. H. Photoassisted construction of holey defective g-C₃N₄ photocatalysts for efficient visible-light-driven H₂O₂ production. *Small* **2018**, 1703142–1703150.
- (25) Tian, J.; Wang, D.; Li, S. T.; Pei, Y.; Qiao, M. H.; Li, Z. H.; Zhang, J. L.; Zong, B. N. KOH-assisted band engineering of polymeric carbon nitride for visible light photocatalytic oxygen reduction to hydrogen peroxide. *ACS Sustainable Chem. Eng.* **2020**, 8, 594–603.